Modeling the Endosomal Escape of Cell-Penetrating Peptides: Transmembrane pH Gradient Driven Translocation across Phospholipid Bilayers†

Mazin Magzoub,‡ Aladdin Pramanik,§ and Astrid Gräslund*,‡

Department of Biochemistry and Biophysics, Stockholm University, S-106 91 Stockholm, Sweden, and Department of Medical Biochemistry and Biophysics, Karolinska Institute, S-171 77 Stockholm, Sweden

Received July 13, 2005; Revised Manuscript Received September 9, 2005

ABSTRACT: Cell-penetrating peptides (CPPs) are able to mediate the efficient cellular uptake of a wide range of cargoes. Internalization of a number of CPPs requires uptake by endocytosis, initiated by binding to anionic cell surface heparan sulfate (HS), followed by escape from endosomes. To elucidate the endosomal escape mechanism, we have modeled the process for two CPPs: penetratin (pAntp) and the N-terminal signal peptide of the unprocessed bovine prion protein (bPrPp). Large unilamellar phospholipid vesicles (LUVs) were produced encapsulating either peptide, and an ionophore, nigericin, was used to create a transmembrane pH gradient (ΔpH_{mem}, inside acidic) similar to the one arising in endosomes in vivo. In the absence of ΔpH_{mem}, no pAntp escape from the LUVs is observed, while a fraction of bPrPp escapes. In the presence of ΔpH_{mem}, a significant amount of pAntp escapes and an even higher degree of bPrPp escape takes place. These results, together with the differences in kinetics of escape, indicate different escape mechanisms for the two peptides. A minimum threshold peptide concentration exists for the escape of both peptides. Coupling of the peptides to a cargo reduces the fraction escaping, while complexation with HS significantly hinders the escape. Fluorescence correlation spectroscopy results show that during the escape process the LUVs are intact. Taken together, these results suggest a model for endosomal escape of CPPs: ΔpH_{mem}-mediated mechanism, following dissociation from HS of the peptides, above a minimum threshold peptide concentration, in a process that does not involve lysis of the vesicles.

The discovery of a class of peptides with the ability to mediate the noninvasive and efficient import of a whole host of cargoes, both in vitro and in vivo, has provided a new means by which the problem associated with the cellular delivery of pharmacologically active compounds for therapeutic purposes can be circumvented (*1*, *2*). The nature of the uptake mechanism of these so-called cell-penetrating peptides (CPPs)[1] remains a hotly debated area, although most recent evidence points to a largely endocytotic uptake for most CPPs, initiated by binding to anionic cell surface glycoaminoglycans, such as heparan sulfate (HS), as well as possibly to other negatively charged moieties on the cell surface, including negatively charged phospholipids and sialic acid (*2*). Macropinocytosis, a rapid, receptor-independent, lipid raft-dependent form of endocytosis, has been implicated (*3*−*5*). In some cases, however, alternative and possibly competing translocation mechanisms also appear to be in operation for CPPs in tandem (*2*, 6).

An important question concerns the means by which endocytosed CPPs (alone or together with a cargo) are able to escape from endosomes or macropinosomes and enter the cytosol in order to modulate cellular functions as efficiently and effectively as has been reported. Currently little is known of the nature of this escape mechanism, apart from that it involves endosome acidification (*7*−*9*). To shed further light on the endosomal escape mechanism, we have modeled the process for two CPPs: penetratin (pAntp), the archetypal CPP with a sequence corresponding to the third helix of the Antennapedia homeodomain (RQIKIWFQNRRMKWKK) (*1*), and the N-terminus of the unprocessed bovine PrP (residues 1−30: MVKSKIGSWILVLFVAMWSDVGLCKKRPKP), denoted bPrPp, which was recently shown to function as a CPP (Magzoub et al., unpublished observations). This peptide also gives rise to membrane perturbation and leakage effects similar to those of the well-characterized pore-forming peptide melittin (derived from bee venom), although higher concentrations of bPrPp are required (*10*). Previously, we had shown that the corresponding sequence from the mouse PrP (residues 1−28, denoted mPrPp) functions as a CPP (*11*). The bPrPp and mPrPp sequences are similar to those of certain chimeric peptides composed of signal sequences and NLS moieties, which are able to efficiently translocate into various cells, even with a conjugated hydrophilic cargo (*2*).

† This work was supported by grants from the Swedish Research Council and from the EU program, Contracts HPRN-CT-2001-00242 and QLK3-CT-2002-01989.

* To whom correspondence should be addressed. Phone: +46-8-162450. Fax: +46-8-155597. E-mail: astrid@dbb.su.se.

‡ Stockholm University.

§ Karolinska Institute.

[1] Abbreviations: CPPs, cell-penetrating peptides; pAntp, penetratin or Antennapedia homeodomain-derived CPP; PrP, prion protein; bPrPp, peptide with sequence corresponding to the N-terminus of the bovine prion protein, residues 1−30; fl-peptides, fluorescein-labeled peptides; Trp, tryptophan; ΔpH_{mem}, transmembrane pH gradient; HS, heparan sulfate; DPPC, 1,2-dipalmitoyl-*sn*-glycero-3-phosphocholine; Chol, cholesterol; SM, sphingomyelin; LUVs, large unilamellar phospholipid vesicles; NLS, nuclear localization sequence; Rh, rhodamine; RLVs, Rh-labeled LUVs; FCS, fluorescence correlation spectroscopy.

10.1021/bi051356w CCC: $30.25
Published on Web 10/21/2005

Large unilamellar phospholipid vesicles (LUVs) were produced encapsulating the CPPs (alone or complexed to HS or coupled to a cargo in the form of the fluorophore fluorescein) and exhibiting a transmembrane salt gradient. The LUVs were composed of DPPC/Chol/SM at a molar ratio of 50/30/20, to mimic the composition of macropinosomes, which in turn reflect the composition of lipid rafts (*12*). Cholesterol, in particular, appears to be of importance to macropinocytosis, since treatment with β-cyclodextrin or nystatin, to deplete or sequester cholesterol, results in inhibition of the process (*3*, *5*). Although lacking the proteins, glycolipids, or coating carbohydrates that are found in cellular membranes, model membrane systems provide a valuable means of studying the membrane interactions of peptides on a molecular level. Furthermore, model membranes allow for the manipulation of the various membrane parameters without possible risking of any interfering reactions that may occur in cellular membranes. LUVs (100 nm diameter) are perhaps the most appropriate model systems currently at our disposal for such a study. LUVs are considerably larger than small unilamellar phospholipid vesicles (SUVs; 30 nm diameter); consequently, the membranes of LUVs have smaller curvature, and experience lesser tension, than the bilayers of SUVs. At the same time, LUVs are more stable than giant unilamellar vesicles (GUVs; diameter >1 μm) whose membranes are rather dynamic, with a tendency to undulate (*13*).

An ionophore, nigercin (*14*), was used to move protons into the LUVs, lowering the internal pH to 5.5 (compared to 7.4 in the external solution) and creating a transmembrane pH gradient, ΔpH_{mem}, similar to the one that arises in endosomal compartments, particularly late endosomes, in vivo (*15*). LUVs exhibiting a transmembrane salt gradient (e.g., entrapping a K^+ salt) will experience an outward movement of entrapped ion coupled to the inward movement of protons when the ionophore nigericin is present at the membrane (*16*). By observing either quenching of the intrinsic tryptophan (Trp) fluorescence or dequenching of the fluorescence intensity of the fluorescein label, due to quencher in the external solution or entrapped in the vesicles, respectively, we determined the fraction of peptide escaping. Additionally, the integrity of the vesicles during the escape process was assessed using FCS. The results of this study give further insight into the currently unexplained mechanism of endosomal escape of CPPs.

EXPERIMENTAL PROCEDURES

Materials. The bovine prion peptide (bPrPp) and penetratin (pAntp) were produced by Neosystem Laboratoire, Strasbourg. Both peptides were C-terminally amidated. Peptides were used as purchased. The identity and purity were controlled by amino acid, mass spectral, and HPLC analyses. Peptides were of immunograde quality (purity estimated at ~80%). In each case peptides from more than one batch were used. Heparan sulfate (HS, estimated MW ~5 kDa, and each HS molecule has approximately 65 negative charges) was purchased from Innovagen AB, Sweden. Nigericin was obtained from Sigma. DPPC (1,2-dipalmitoyl-*sn*-glycero-3-phosphocholine), cholesterol, and sphingomyelin (brain) were all from Avanti Polar Lipids, Alabaster, of the best quality, and were used without further purification. Rh-PE (6-tetramethylrhodamine-1,2-dihexadecanoyl-3-phosphoethanolamine) was obtained from Molecular Probes, The Netherlands.

Determination of Peptide Concentrations. After the peptides were weighed on a microbalance, the peptide concentrations in the stock solutions were determined by light absorption on a CARY 4 UV−visible spectrophotometer, using 1 cm optical quartz cuvettes. All of the spectra were baseline corrected. Molar absorptivities of 5690 and 1280 M^{-1} cm^{-1}, at 280 nm, for tryptophan and tyrosine, respectively, were applied (*17*).

Steady-State Fluorescence Spectroscopy. Fluorescence was measured on a JOBIN YVON Fluorolog-3 spectrofluorometer. Measurements were made in 4×10 mm quartz cuvettes at 20 °C. The intrinsic Trp fluorescence of the peptides was excited at 280 nm and the emission wavelength scanned from 300 to 400 nm. For fl-peptide experiments, the excitation of the fluorescein label was at 492 nm and the emission scanned from 510 to 600 nm. Scans were usually recorded with 2 nm excitation and emission bandwidths and a scan speed of 250 nm/min. Three scans were recorded and averaged for each sample.

Interaction of pAntp with Heparan Sulfate (HS). Increasing concentrations of HS were added to fl-peptide (final concentration 1.25 μM) in PBS in a 4×10 mm cuvette. Following incubation of the samples for 30 min, at 20 °C, the fluorescence of the fluorescein label was recorded. The background signal of HS alone was recorded separately for the same titration and subtracted. The fluorescence was plotted as a function of [HS]/[peptide].

Preparation of LUVs. Large unilamellar vesicles were prepared by initially dissolving the phospholipids DPPC/Chol/SM (50/30/20) in a chloroform/ethanol mixture, to ensure complete mixing of the components, and then removing the solvent by placing the sample in a high vacuum for 3 h. The dried lipids were dispersed in a salt solution [300 mM K_2SO_4 (pH 7.4)]. The dispersion was run through a freeze−thaw cycle five times and then passed through two polycarbonate filters (0.1 μm pore size) 20 times in an Avanti manual extruder (*18*).

Assays for Peptide Escape. Two complementary assays were used to determine the escape of the peptides from the vesicles in the presence of ΔpH_{mem} (inside acidic). The phospholipids were dissolved in the salt solution also containing nonlabeled peptide alone or complexed to HS (following co-incubation for 30 min) or fl-peptide plus KI (from a 1 M stock solution) as quencher. LUVs were then prepared as described earlier and passed through a PD-10 column (Amersham Biosciences, Uppsala, Sweden) equilibrated with 300 mM sucrose plus 20 mM HEPES (pH 7.4), resulting in the removal of external metal ions and peptide (and quencher) and creation of a transmembrane salt gradient. Nigericin (from a 10 mM ethanolic stock solution) alone, in the case of fl-peptides, or nigericin plus the quencher acrylamide (from a 1 M stock solution), in the case of nonlabeled peptides, was then added to the eluted LUVs, and the fluorescence of the sample was immediately recorded. The ionophore nigericin catalyzes the electroneutral one-for-one exchange of H^+ for K^+ across the LUV membrane, thereby lowering the internal pH. This nigericin treatment creates a ΔpH_{mem} of 2−3 units (i.e., the internal pH is ~5.5) (*16*).

The amount of peptide escaping was determined from either quenching of the peptide intrinsic Trp fluorescence (in the case of the nonlabeled peptides) or dequenching of the fluorescein label (in the case of fl-peptides). The fluorescence intensity corresponding to 100% peptide escape (F_{max}) was determined by lysing the vesicles with 10% (w/v) Triton X-100. The percent peptide escape was then calculated according to the equation:

$$\% \text{ escape} = 100\left(\frac{F_T - F_0}{F_{max} - F_0}\right) \quad (1)$$

where F_0 represents the fluorescence intensity of the vesicles at the start of recording of the experiment ($t = 0$) and F_T the intensity at measured time ($t = T$).

Monitoring Nigericin Action Using Phenol Red. DPPC/Chol/SM (50/30/20) was dispersed in a 300 mM K_2SO_4 solution containing 100 μM phenol red (from a 10 mM stock solution). LUVs were prepared as described earlier, and external phenol red was removed by passing the LUVs through a PD-10 column equilibrated with HEPES-buffered sucrose. Nigericin was then added to create ΔpH_{mem}, and the absorbance of the encapsulated phenol red was monitored at 557 nm as a function of time on a CARY 4 UV−visible spectrophotometer.

FCS Instrumentation and Data Evaluation. FCS was performed with confocal illumination of a volume element of 0.2 fl in an instrument as described previously (*19*, *20*). As focusing optics a Zeiss Neofluar 63 × NA 1.2 was used in an epi-illumination setup. For separating exciting from emitted radiation, a dichroic filter (Omega 540 DRL PO2) and a band-pass filter (Omega 565 DR 50) were used. Rh-labeled LUVs (RLVs) were excited with the 514.5 nm line of an argon laser. The fluorescence intensity fluctuations were detected by an avalanche photodiode (EG & SPCM 200) and were correlated with a digital correlator (ALV 5000; ALV, Langen, Germany). The FCS parameters, including the diffusion time, τ_D, were analyzed as previously described (*10*).

Assessing LUV Integrity during Peptide Escape. To prepare the Rh-labeled LUVs (RLVs), the phospholipids, including 0.1 mol % Rh-labeled lipids, were dissolved in the chloroform/ethanol mixture prior to making the lipid film. The phospholipids were then dispersed in the 300 mM K_2SO_4 solution containing the nonlabeled peptide, and the RLVs were prepared and ΔpH_{mem} was created as described previously.

Free Rh was used as a reference to calibrate the instrument and to estimate diffusion times of the RLVs, as well as to determine whether the vesicles are intact or destroyed. The diffusion times of free Rh and RLVs were determined separately. The integrity of the vesicles during the escape process was assessed. Since Rh is covalently bound to the headgroups of the phosphatidylethanolamine, only the disintegration of the RLVs can lead to the appearance of faster diffusing Rh in solution. Samples were taken at several points of incubation, ranging from minutes to hours, and analyzed in the FCS instrument from 30 s up to 10 min.

RESULTS

Interaction of pAntp with Heparan Sulfate (HS) Free in Solution. To investigate the nature of interaction between the peptides and HS, fl-peptides were titrated with HS in solution (Figure 1). Increasing amounts of HS caused fluorescence quenching of the fluorescein label, due to formation of complexes composed of HS and peptide. Since HS has −65 charges per molecule, and from a peptide charge of +7 and +5 per molecule for pAntp and bPrPp, respectively, electrically neutral complexes are estimated to correspond to a molar ratio, [HS]/[peptide], of ∼ 0.11 and 0.08 for pAntp and bPrPp, respectively. From Figure 1 it can be seen that it is only at higher concentrations of HS than corresponding to the points of electroneutrality that the quenching becomes pronounced for the peptides. For the same HS concentration, a greater degree of quenching is observed for pAntp compared to bPrPp, up to [HS]/[peptide] ∼ 0.6, possibly a reflection of the higher number of charges on pAntp. However, at the final point of titration, the initial fluorescence decreased to around 40% for pAntp, compared to around 20% for bPrPp, probably due to formation of larger or more compact aggregates in the case of bPrPp. A partial reversal of the process, around 50% only of the fluorescence signal was recovered, was induced by addition of high concentrations of NaCl (∼2 M) (data not shown), indicating that the electrostatic complexes are highly stable.

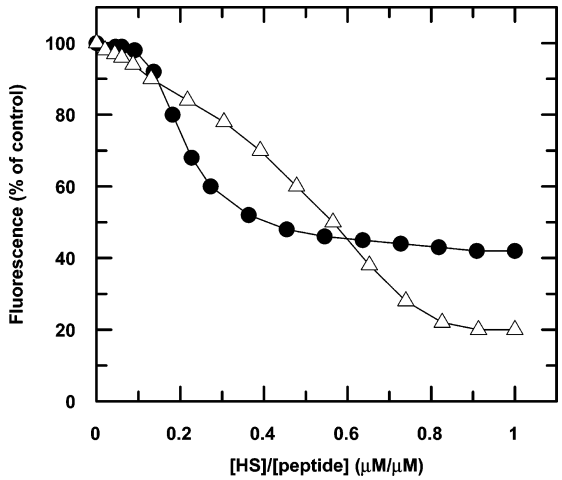

FIGURE 1: Quenching of fluorescein-labeled peptides (fl-peptides) by heparan sulfate (HS) in solution. Increasing concentrations of HS were added to a solution of fl-pAntp (●) or fl-bPrPp (△) in PBS (final peptide concentration was 1.25 μM). Following incubation for 30 min, the fluorescence intensity of the fluorescein label was recorded at 20 °C and then plotted, after background correction, as a function of [HS]/[peptide].

The kinetics of complex formation (quenching) for both peptides exhibits two phases: a rapid one which has a duration of seconds and accounts for approximately 80% of the quenching, followed by a second, much slower phase in which there is a continued decrease of fluorescence over 15 min (data not shown).

ΔpH_{mem}-Mediated Escape of Peptides from LUVs. The escape of the encapsulated nonlabeled peptides (at a concentration of 20 μM) from the LUVs (100 μM total lipid concentration), determined from quenching of their intrinsic Trp fluorescence and quantified using eq 1, is shown in Figure 2. In the absence of ΔpH_{mem}, practically no pAntp escape is observed (∼3%) while in the presence of the ΔpH_{mem}, approximately 25% of the peptide escapes (Figure 2a). Complexation of the peptide to HS, at [HS]/[peptide] = 0.6, leads to a lower fraction of peptide escaping (∼10%)

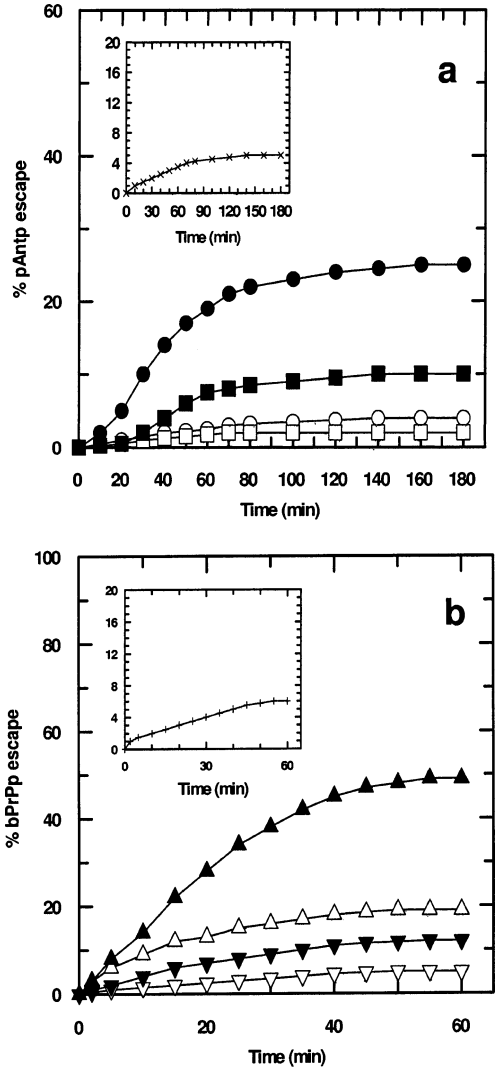

FIGURE 2: Escape of nonlabeled peptides from LUVs. (a) 20 μM pAntp alone in the absence (○) or presence (●) of ΔpH_{mem}; 20 μM pAntp complexed with 12 μM HS ([HS]/[peptide] = 0.6) in the absence (□) or presence (■) of ΔpH_{mem}. Inset: 1 μM pAntp alone in the presence of ΔpH_{mem}. (b) 20 μM bPrPp pAntp alone in the absence (△) or presence (▲) of ΔpH_{mem} or in the presence ΔpH_{mem}; 20 μM bPrPp complexed with 12 μM HS ([HS]/[peptide] = 0.6) in the absence (▽) or presence (▼) of ΔpH_{mem}. Inset: 1 μM bPrPp alone in the presence of ΔpH_{mem}. The LUVs were composed of DPPC/Chol/SM (50/30/20), with a total lipid concentration of 100 μM. Escape was monitored through quenching of the intrinsic Trp fluorescence by 100 mM acrylamide in the external solution. The $t = 0$ point is defined as the time immediately after elution of the LUVs, which is also when nigericin is added for the experiments with ΔpH_{mem}. The escape was quantified using eq 1. The spectra were recorded at 20 °C.

in the presence of the pH gradient. The escape process, which has a total duration of 3 h, is biphasic with the first, more rapid, phase taking up to 70 min and accounting for almost 90% of the escape, while the remainder takes place over the following 110 min.

In the case of bPrPp, a certain fraction of the peptide is able to escape (~20%) in the absence of ΔpH_{mem}, while the introduction of the pH gradient increases the fraction more than 2-fold to 50% (Figure 2b). Once more, complexation of the peptide to HS, also at [HS]/[peptide] = 0.6, hinders the escape (~10% escaping, in the presence of ΔpH_{mem}). A more rapid escape takes place for bPrPp (total duration ~60 min) than for pAntp (Figure 2a), although the process is again

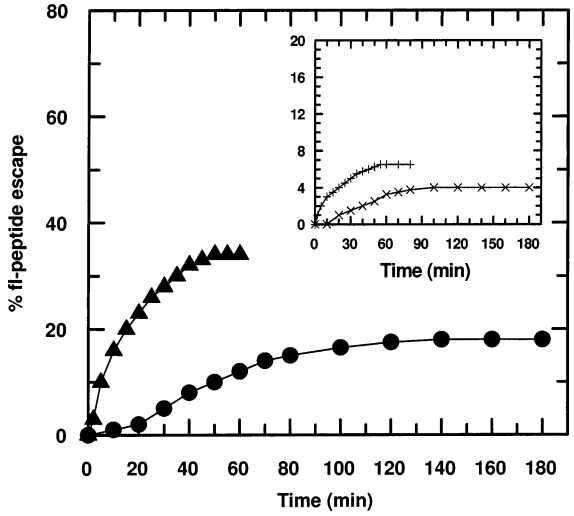

FIGURE 3: Escape of fluorescein-labeled peptides (fl-peptides) from LUVs. DPPC/Chol/SM (50/30/20) LUVs (with a total lipid concentration of 100 μM) encapsulating 20 μM fl-pAntp (●) or fl-bPrPp (▲), as well as 50 mM KI as quencher, in the presence of ΔpH_{mem}. Inset: 1 μM pAntp (×) or 1 μM bPrPp (+) in the presence of ΔpH_{mem}. Escape was monitored by the increase in fluorescence of the fluorescein label due to dequenching. Time $t = 0$ is again defined as immediately after elution of the LUVs when nigericin is added to the solution. Escape was quantified using eq 1. The spectra were recorded at 20 °C.

biphasic, with a steady increase over the first 40 min accounting for 90−95% of the escape, which then levels off over the next 20 min.

Figure 3 shows the escape of the fl-peptides from the LUVs, determined from dequenching of the fluorescein label and quantified using eq 1. Again, a larger degree of escape is observed for fl-bPrPp than fl-pAntp (approximately 35% and 20%, respectively), although for both peptides this is lower than observed with the nonlabeled peptides (Figure 2), possibly indicating that the fluorescein label hinders the escape. At the lower concentrations of peptides (1 μM) no significant escape is observed, either for nonlabeled or labeled peptides (Figures 2a,b and 3, insets). For both peptides, any observed increase (in the case of the nonlabeled peptides), or decrease (in the case of the fl-peptides), in the fluorescence intensity that takes place is permanent. This indicates that once they escape from the vesicles, the peptides remain in the external solution; i.e., the peptides do not flip-flop from inside to out and vice versa.

To ensure that the increase in the fluorescence intensity of the fl-peptides is not simply due to peptide bound on the outer surface of the vesicles dissociating as a result of binding of nigericin, prior to addition of nigericin, a large amount of KI (1 M) was added to the external solution to quench any external peptide. No change in fluorescence intensity was observed, indicating that no peptide resides on the outer surface of the vesicles or in the external solution.

As a further control, the effect of pH on the fluorescence intensity of the fl-peptides in solution was monitored. It was found that the fluorescence intensity of the fluorescein label decreases with lower pH (~50−60% decrease in intensity observed at pH 5.5). Therefore, the increase in fluorescence intensity observed for the fl-peptides during the peptide escape experiments cannot be due to changes in quantum yield of the fluorescein label in response to the changes in pH and can only be explained by escape of the peptide from

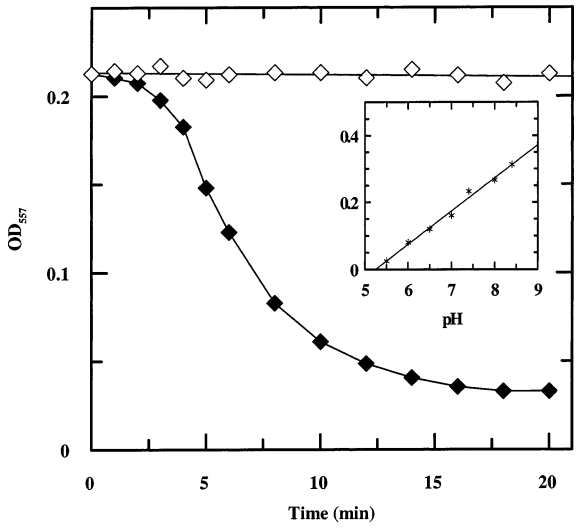

FIGURE 4: Changes in phenol red absorbance as a function of time. The change in absorbance at 557 nm of 100 μM phenol red entrapped in DPPC/Chol/SM (50/30/20) LUVs (with a total lipid concentration of 100 μM) in response to protons being moved into the LUVs by the ionophore nigericin (◆). As a control, the absorbance of entrapped phenol red is monitored in the absence of nigericin (◇). Time $t = 0$ is defined as the point at which nigericin (or an equal volume of buffer in the control experiment) is added to the solution. Inset: calibration curve obtained by measuring absorbance of 100 μM phenol red at 557 nm in solutions of different pH (line represents a linear fit of the points). To correct for concentration differences, the absorbance in a solution of pH 7.4 was adjusted to match the initial absorbance of LUV-entrapped phenol red. The absorbance was recorded at an ambient temperature (20 °C).

the lumen of the LUVs, where both a lower pH and a high concentration of quencher, KI, exist.

Monitoring Nigericin Action Using Phenol Red. The sensitivity of phenol red absorbance to changes in pH of the environment (*21*) was used to verify that nigericin is indeed moving protons into the LUVs in the peptide escape assays. Figure 4 shows the change in the absorbance of the encapsulated phenol red at 557 nm as a function of time. The absorbance decreased over a period of 20 min from approximately 0.21 to 0.04. From a calibration curve, in which the absorbance of phenol red was measured at 557 nm in solutions of different pH (Figure 4, inset), this miminum absorbance was determined to correspond to a pH of ~5.5. This confirms that in the peptide escape experiments nigericin creates a ΔpH_{mem} of ~2 units (inside acidic).

Integrity of LUVs during Peptide Escape. FCS was used to assess the integrity of the LUVs during the peptide escape process (Figure 5). The diffusion time, τ_D, for free Rh in solution is ~0.07 ± 0.002 ms (Figure 5a), while for RLVs (with a 100 μM total lipid concentration) entrapping 20 μM pAntp or bPrPp, in the presence of ΔpH_{mem}, a much longer τ_D is observed (8.1 ± 1 ms), even following incubation for 3 h (Figure 5b,c, respectively). This value is in good agreement with the τ_D obtained in a previous study for RLVs (*22*). In contrast, lysing the RLVs entrapping pAntp (Figure 5d), or bPrPp (data not shown), by adding 10% (w/v) Triton X-100, leads to a sharp decrease in the average τ_D to ~0.13 ± 0.04 ms (Figure 5d). Hence, the escape mechanism of the peptides does not involve lysis of the vesicles, although we cannot discount the possibility that the integrity of the vesicles is compromised to a lesser extent, which is not reflected by a change in the value of τ_D.

DISCUSSION

Endocytosis has been shown to play a significant role in the cellular internalization of a large number of CPPs, although there is evidence suggesting the existence of other, perhaps competing, uptake mechanisms (*2*, *6*). In the case of endocytosis, the internalization is essentially a two-step process: uptake by endocytosis (lipid raft-mediated macropinocytosis) initiated by binding to cell surface HS but also possibly negatively charged phospholipids and sialic acid, followed by escape from endosomes (macropinosomes) (*3*−*5*). Currently, little is known about the nature of the endosomal escape of CPPs. Recent studies indicate that the mechanism involves endosome acidification (from pH 7.4 to pH 5.5) prior to the endosome reaching the lysosome, thereby evading degradation (*7*−*9*).

To shed further light on the endosomal escape mechanism(s), we have modeled the process using LUVs composed of DPPC/Chol/SM (50/30/20), encapsulating the CPPs pAntp or bPrPp, and exhibiting a transmembrane salt gradient. The ionophore nigericin was used to lower the internal LUV pH to ~5.5 (compared to an external pH of 7.4), thereby creating a similar ΔpH_{mem} to the one experienced by endosomes in vivo (*15*). The results show that in the absence of ΔpH_{mem} virtually no pAntp escape takes place (Figure 2a), while a significant degree of bPrPp escape is observed (Figure 2b). In the presence of ΔpH_{mem} the fraction escaping is enhanced considerably for both peptides, although the amount of bPrPp escaping is again much higher (Figure 2). Moreover, the kinetics of escape is different for the two peptides, with a faster rate observed for bPrPp (Figure 2). These results suggest two partially different escape mechanisms in operation for the two CPPs.

In the absence of ΔpH_{mem}, the propensity of bPrPp to form transient pores, driven by the peptide concentration gradient, could account for the observed escape (*10*). The enhancement of escape as a result of ΔpH_{mem} could be due to a mechanism similar to that of the pH-sensitive endosomal escape of certain types of viruses, including adenoviruses (*23*, *24*). In that case, the acidic environment of endosomes leads to protonation of the acidic residues, aspartic acid and glutamic acid, within peptide regions of the adenovirus. This increases the hydrophobicity of these regions, enhancing the viral protein's interaction with the endosomal membrane, where it forms pores or lyses the membrane, allowing the viral genome to enter the cytoplasm (*25*−*27*). Similarly, protonation of the aspartic acid of bPrPp at the lower pH leads to a longer hydrophobic stretch within the peptide sequence, which may enhance the membrane interaction, leading to a higher degree of pore formation and escape. Pore formation as the likely escape route is supported by the observation that the escape is not accompanied by lysis of the vesicles (Figure 5) and is also in agreement with our previous observations (*10*) that bPrPp has a similar mode of membrane interaction as melittin, known to form pores in bilayers (*28*, *29*).

In the case of pAntp, the peptide concentration gradient alone is not enough to drive the escape. However, the nature of the ΔpH_{mem}-mediated escape mechanism, which again

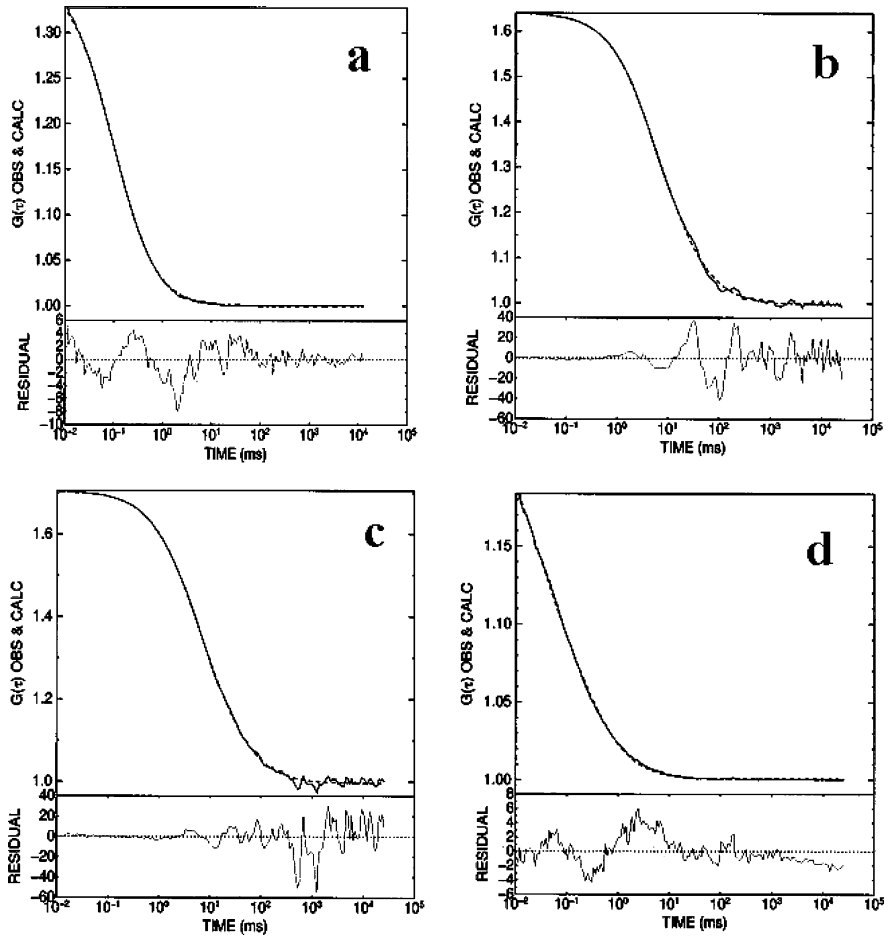

FIGURE 5: Integrity of the LUVs during the escape process as determined by FCS. The fluorescence intensity autocorrelation functions, $G(\tau)$, of (a) free rhodamine (Rh) in solution, Rh-labeled LUVs (RLVs) entrapping 20 μM (b) pAntp or (c) bPrPp, in the presence of ΔpH_{mem}, following incubation for 3 h, and (d) RLVs entrapping pAntp following addition of 10% (w/v) Triton X-100. The composition of the RLVs was DPPC/Chol/SM (50/30/20), with a total lipid concentration of 100 μM. All spectra were recorded at an ambient temperature (20 °C).

does not involve lysis of the membrane (Figure 5), is not immediately apparent since the peptide does not form pores (*1*), nor does it have any amino acids that are sensitive to pH changes. A possibility is that membrane depolarization, resulting from the inward movement of protons, drives the membrane insertion of the peptide, followed by escape. A similar effect has been described for the voltage-sensor paddle domains, which contain four or more evenly spaced charged amino acids, of voltage-dependent K^+ channels (*30*, *31*). A change in the orientation of the paddle domain in response to membrane voltage takes place, resulting in movement of the gating charges or charged amino acids located on the paddle across the membrane near the protein−lipid interface. Although the energetic cost of burying charges in a lipid bilayer would appear to prohibit such a mechanism (*32*), it was recently determined that factors such as the relative positioning of the charged residues within the sequence contribute to the free energy of membrane insertion (*33*). Thus, depending on the location of the cationic amino acids, a rather charged sequence can be accommodated in a lipid bilayer.

Alternatively, it is possible that the escape mechanism of pAntp involves the induction of another lipid phase, such as the hexagonal lipid phase, i.e., the formation of so-called "inverted micelles". It has been previously reported that pAntp induces the formation of such a phase within the lipid bilayer, through which the peptide may cross the membrane without disruption of its integrity (*6*).

There appears to be a threshold peptide concentration below which no significant escape is observed (Figures 2 and 3, insets). This is in agreement with the observation that a minimum CPP concentration is required for a biological effect of a coupled cargo to be observed (*2*). For pAntp it is possible that a minimum peptide concentration gradient is required to facilitate the ΔpH_{mem}-driven membrane insertion of the peptide followed by its escape. In the case of bPrPp, this can be explained in terms of a minimum threshold peptide concentration required for pore formation leading to escape. The dependence of pore formation on peptide concentration has been proposed for several host-defense peptides (i.e., toxins and antimicrobial peptides), including melittin (*34*−*36*).

For both peptides stable complexation with HS significantly hinders the escape (Figure 2). The ratio, [HS]/[peptide] = 0.6, was chosen as it gives the same degree of quenching for both fl-peptides (∼50%), suggesting similarly sized complexes (Figure 1). Interestingly for both peptides, complexation resulted in approximately the same low fraction escaping (∼10%) (Figure 2). These results indicate that dissociation of the peptide from HS is a prerequisite for endosomal escape, which in vivo would take place due to hydrolytic degradation of HS by heparanases en route to the

lysosome (*37*). Additionally, the coupling of the peptides to a cargo, in the form of a fluorescence label (fluorescein), leads to a reduction in the fraction of peptide escaping (Figure 3). It has previously been suggested that the size of a delivered molecule could have a major impact on its mechanism of internalization and the subsequent intracellular routing (*38*, *39*). More recently, it was found that attachment of a cargo to a CPP reduces the uptake efficiency and leads to a higher fraction retained in endosomal compartments (*40*).

In a recent study, the true amount of peptide that reaches the cytosol as opposed to peptide bound to the membrane and entrapped in endosomes was assessed using a functional assay involving the delivery of an apoptosis-inducing peptide (proapoptotic domain peptide, PAD) coupled to oligoarginine CPPs (*4*). Assessing the apoptotic cell death, it was determined that no more than 20−30% of internalized peptides escaped to the cytosol. This value agrees quite well with the values obtained in this study. Moreover, that study further highlights the fact that endosomal escape is the rate-limiting step for peptide translocation into the cytoplasm.

In conclusion, taken together, the results of this study suggest a model for the internalization of a number of CPPs: interaction with HS at the cell surface to form stable complexes; uptake by endocytosis leading to the complexes residing in endosomes; dissociation of the complexes by heparanases; endosomal ΔpH_{mem}-mediated escape of internalized peptide, above a minimum threshold peptide concentration, through a mechanism that does not involve lysis of the vesicles.

ACKNOWLEDGMENT

We thank L. E. Göran Eriksson for valuable discussions. We also thank Henrik Biverståhl and Jörgen Björklund for help with the phenol red measurements.

REFERENCES

1. Langel, Ü., Ed. (2002) *Cell-Penetrating Peptides. Processes and Applications*, CRC Press, Boca Raton, FL.
2. Magzoub, M., and Gräslund, A. (2004) Cell-penetrating peptides: from inception to application, *Q. Rev. Biophys. 37*, 147−195.
3. Wadia, J. S., Stan, R. V., and Dowdy, S. F. (2004) Transducible Tat-HA fusogenic peptide enhances escape of Tat-fusion proteins after lipid raft macropinocytosis, *Nat. Med. 10*, 310−315.
4. Nakase, I., Niwa, M., Takeuchi, T., Sonomura, K., Kawabata, N., Koike, Y., Takehashi, M., Tanaka, S., Ueda, K., Simpson, J. C., Jones, A. T., Sugiura, Y., and Futaki S. (2004) Cellular uptake of arginine-rich peptides: roles for macropinocytosis and actin rearrangement, *Mol. Ther. 10*, 1011−1022.
5. Foerg, C., Ziegler, U., Fernandez-Carneado, J., Giralt, E., Rennert, R., Beck-Sickinger, A. G., and Merkle, H. P. (2005) Decoding the entry of two novel cell-penetrating peptides in HeLa cells: lipid raft-mediated endocytosis and endosomal escape, *Biochemistry 44*, 72−81.
6. Joliot, A., and Prochiantz, A. (2004) Transduction peptides: from technology to physiology, *Nat. Cell Biol. 6*, 189−196.
7. Potocky, T. B., Menon, A. K., and Gellman, S. H. (2003) Cytoplasmic and nuclear delivery of a Tat-derived peptide and a β-peptide after endocytotic uptake into HeLa cells, *J. Biol. Chem. 278*, 50188−50194.
8. Koch, A. M., Reynolds, F., Kircher, M. F., Merkle, H. P., Weissleder, R., and Josephson, L. (2003) Uptake and metabolism of a dual fluorochrome Tat-nanoparticle in HeLa cells, *Bioconjugate Chem. 14*, 1115−1121.
9. Fischer, R., Köhler, K., Fotin-Mleczek, M., and Brock, R. (2004) A stepwise dissection of the intracellular fate of cationic cell-penetrating peptides, *J. Biol. Chem. 279*, 12625−12635.
10. Magzoub, M., Oglecka, K., Pramanik, A., Eriksson, L. E. G., and Gräslund, A. (2005) Membrane perturbation effects of peptides derived from the N-termini of unprocessed prion proteins, *Biochim. Biophys. Acta* (in press).
11. Lundberg, P., Magzoub, M., Lindberg, M., Hällbrink, M., Jarvet, J., Eriksson, L. E. G., Langel, Ü., and Gräslund, A. (2002) Cell membrane translocation of the N-terminal (1−28) part of the prion protein, *Biochem. Biophys. Res. Commun. 299*, 85−90.
12. Swanson, J. A., and Watts, C. (1995) Macropinoytosis, *Trends Cell Biol. 5*, 424−428.
13. Fischer, A., Oberholzer, T., and Luisi P. L. (2000) Giant vesicles as models to study the interactions between membranes and proteins, *Biochim. Biophys. Acta 1467*, 177−188.
14. Deamer, D. W., Prince, R. C., and Crofts, A. R. (1972) The response of fluorescent amines to pH gradients across liposome membranes, *Biochim Biophys. Acta 274*, 323−335.
15. Gruenberg, J. (2001) The endocytic pathway: a mosaic of domains, *Nat. Rev. Mol. Cell. Biol. 2*, 721−730.
16. Fenske, D. B., Wong, K. F., Maurer, E., Maurer, N., Leenhouts, J. M., Boman, N., Amankwa, L., and Cullis, P. R. (1998) Ionophore-mediated uptake of ciprofloxacin and vincristine into large unilamellar vesicles exhibiting transmembrane ion gradients, *Biochim. Biophys. Acta 1414*, 188−204.
17. Gill, S. C., and von Hippel, P. H. (1989) Calculation of protein extinction coefficients from amino acid sequence data, *Anal. Biochem. 182*, 319−326.
18. Mayer, L. D., Hope, M. J., and Cullis, P. R. (1986) Vesicles of variable sizes produced by a rapid extrusion procedure, *Biochim. Biophys. Acta 858*, 161−168.
19. Rigler, R., and Mets, Ü. (1993) Diffusion of single molecules through a Gaussian laser beam, *Soc. Photo-Opt. Instrum. Eng. 1921*, 239−248.
20. Rigler, R., Widengren, J., and Mets, Ü. (1992) Interactions and kinetics of single molecules as observed by fluorescence correlation spectroscopy, in *Fluorescence Correlation Spectroscopy* (Wolfbeis, O. J., Ed.) pp 13−24, Springer-Verlag, Berlin.
21. Deng, C., and Chen, R. R. (2004) A pH-sensitive assay for galactosyltransferase, *Anal. Biochem. 330*, 219−226.
22. Pramanik, A., Thyberg, P., and Rigler, R. (2000) Molecular interactions of peptides with phospholipids vesicle membranes as studied by fluorescence correlation spectroscopy, *Chem. Phys. Lipids 104*, 35−47.
23. Cho, Y. W., Kim, J.-D., and Park, K. (2003) Polycation gene delivery systems: escape from endosomes to cytosol, *J. Pharm. Pharmacol. 55*, 721−734.
24. Meier, O., Boucke, K., Hammer, S. V., Keller, S., Stidwill, R. P., Hemmi, S., and Greber, U. F. (2002) Adenovirus triggers macropinocytosis and endosomal leakage together with its clathrin-mediated uptake, *J. Cell Biol. 158*, 1119−1131.
25. Blumenthal, R., Seth, P., Willingham, M. C., and Pastan, I. (1986) pH-dependent lysis of liposomes by adenovirus, *Biochemistry 25*, 2231−2237.
26. Greber, U. F., Willetts, M., Webster, P., and Helenius, A. (1993) Stepwise dismantling of adenovirus 2 during entry into cells, *Cell 75*, 477−486.
27. Seth, P. (1994) Adenovirus-dependent release of choline from plasma membrane vesicles at an acidic pH is mediated by the penton base protein, *J. Virol. 68*, 1204−1206.
28. Dempsey, C. E. (1990) The actions of melittin on membranes, *Biochim. Biophys. Acta 1031*, 143−161.
29. Matsuzaki, K., Yoneyama, S., and Miyajima, K. (1997) Pore-formation and translocation of melittin, *Biophys. J. 73*, 831−838.
30. Jiang, Y., Ruta, V., Chen, J., Lee, A., and MacKinnon, R. (2003) The principle of gating charge movement in a voltage-dependent K^+ channel, *Nature 423*, 42−48.
31. Long, S. B., Campbell, E. B., and MacKinnon, R. (2005) Voltage sensor of Kv1.2: structural basis of electromechanical coupling, *Science 309*, 903−908.
32. Grabe, M., Lecar, H., Jan, Y. N., and Jan, L. Y. (2004) A quantitative assessment of models for voltage-dependent gating of ion channels, *Proc. Natl. Acad. Sci. U.S.A. 101*, 17640−17645.
33. Hessa, T., Kim, H., Bihlmaier, K., Lundin, C., Boekel, J., Andersson, H., Nilsson, I., White, S. H., and von Heijne, G. (2005) Recognition of transmembrane helices by the endoplasmic reticulum translocon, *Nature 433*, 377−381.
34. Matsuzaki, K., Murase, O., and Miyajima, K. (1995) Kinetics of pore formation by an antimicrobial peptide, magainin 2, in phospholipid bilayers, *Biochemistry 34*, 12553−12559.

35. Yang, L., Harroun, T. A., Weiss, T. M., Ding, L., and Huang, H. W. (2001) Barrel-stave model or toroidal model? A case study on melittin pores, *Biophys. J. 81*, 1475−1485.
36. Zhang, L., Rozek, A., and Hancock, R. E. W. (2001) Interaction of cationic antimicrobial peptides with model membranes, *J. Biol. Chem. 276*, 35714−35722.
37. Yanagishita, M., and Hascall, V. C. (1984) Metabolism of proteoglycans in rat ovarian granulosa cell culture, *J. Biol. Chem. 259*, 10207−10283.
38. Zuhorn, I. S., Visser, W. H., Bakowsky, U., Engberts, J. B., and Hoekstra, D. (2002) Interference of serum with lipoplex-cell interaction: modulation of intracellular processing, *Biochim. Biophys. Acta 1560*, 25−36.
39. Rejman, J., Oberle, V., Zuhorn, I. S., and Hoekstra, D. (2004) Size-dependent internalization of particles via the pathways of clathrin- and caveolae-mediated endocytosis, *Biochem. J. 377*, 159−169.
40. Maiolo, J. R., Ferrer, M., and Ottinger, E. A. (2005) Effects of cargo molecules on the cellular uptake of arginine-rich cell-penetrating peptides, *Biochim. Biophys. Acta 1712*, 161−172.

BI051356W